# Extremal Trajectories for Bounded Velocity Differential Drive Robots

Devin J. Balkcom Matthew T. Mason

Robotics Institute and Computer Science Department
Carnegie Mellon University
Pittsburgh PA 15213

## Abstract

*This paper applies Pontryagin's Maximum Principle to the time optimal control of differential drive mobile robots with velocity bounds. The Maximum Principle gives necessary conditions for time optimality.* Extremal trajectories *are those which satisfy these conditions, and are thus a superset of the time optimal trajectories. The paper derives a compact geometrical structure for extremal trajectories and shows that extremal trajectories are always composed of rotations about the robot center and straight line motions. Further necessary conditions are obtained, and symmetry classes are identified.*

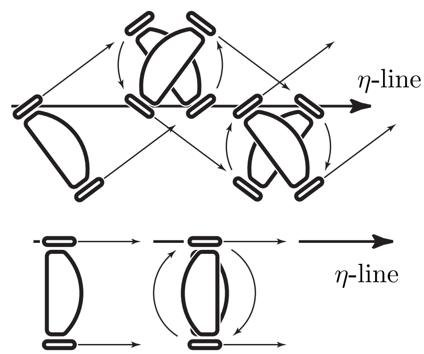


Figure 1: Two extremals: *zigzag right* and *tangent CW*. Other extremal types are *zigzag left*, *tangent CCW*, and turning in place: *CW* and *CCW*. Straight lines are special cases of zigzags or tangents.

## 1 Introduction

This paper focuses on the application of Pontryagin's Maximum Principle to the time optimal control of diff drive mobile robots with velocity bounds. A *diff drive* robot has two independently driven coaxial wheels. By *velocity bounds,* we mean that the wheel velocities are bounded, but there are no bounds on wheel acceleration. In fact, discontinuities in wheel velocity are allowed.

Pontryagin's Maximum Principle yields conditions that are necessary but not sufficient for time optimal trajectory. Hence the trajectories that satisfy the Maximum Principle are called *extremal* trajectories, and are a superset of the time optimal trajectories. The Maximum Principle provides a compact geometrical description of the extremal trajectories, and thus gives us a tool for enumerating and exploring time optimal trajectories. Figure 1 shows two of the six different extremal types.

### 1.1 Previous Work

Although this paper is self-contained, readers interested in the broader issue of time optimal paths should probably begin with our companion paper [1].

There appears to be no previous work on time-optimal control of the bounded velocity diff drive robot, but the techniques employed here are a straightforward extension of the techniques developed for steered vehicles [6, 2, 5, 4].

## 2 Assumptions, definitions, notation

The state of the robot is $q = (x, y, \theta)$, where the robot reference point $(x, y)$ is centered between the wheels, and the robot direction $\theta$ is 0 when the robot is facing along the $x$-axis, and increases in the counterclockwise direction (Figure 2). The robot's velocity in the forward direction is $v$ and its angular velocity is $\omega$. The robot's width is $2b$. The wheel angular velocities are $\omega_l$ and $\omega_r$. With suitable choices of units we obtain

$$v = \frac{1}{2}(\omega_l + \omega_r) \tag{1}$$

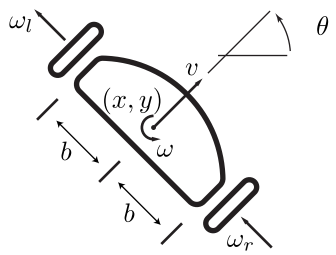


Figure 2: Notation

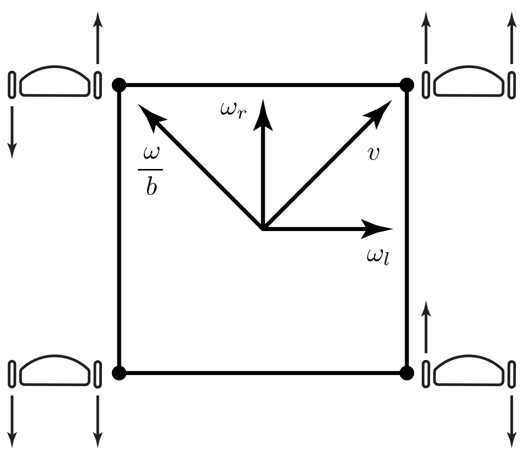


Figure 3: Bounds on $(\omega_l, \omega_r)$

$$\omega = \frac{1}{2b}(\omega_r - \omega_l) \tag{2}$$

and

$$\omega_l = v - b\omega \tag{3}$$
$$\omega_r = v + b\omega \tag{4}$$

The robot is a system with control input $w(t) = (\omega_l(t), \omega_r(t))$ and output $q(t)$. Admissible controls are bounded Lebesgue measurable functions from time interval $[0, T]$ to the closed box $W = [-1, 1] \times [-1, 1]$ (see Figure 3).

It follows immediately that $v(t)$ and $\omega(t)$ are measurable functions defined on the same interval. Given initial conditions $q_s = (x_s, y_s, \theta_s)$ the path of the robot is given by

$$\theta(t) = \theta_s + \int_0^t \omega \tag{5}$$
$$x(t) = x_s + \int_0^t v\cos(\theta) \tag{6}$$
$$y(t) = y_s + \int_0^t v\sin(\theta) \tag{7}$$

It follows that $\theta$, $x$, $y$, and $s$ are continuous, that their time derivatives exist almost everywhere, and that

$$\dot{\theta} = \omega \quad \text{a.e.} \tag{8}$$
$$\dot{s} = v \quad \text{a.e.} \tag{9}$$
$$\dot{x} = v\cos(\theta) \quad \text{a.e.} \tag{10}$$
$$\dot{y} = v\sin(\theta) \quad \text{a.e.} \tag{11}$$

We also need a notation for trajectories. Later sections show that extremal trajectories are composed of straight lines and turns about the robot's center. We will represent *forward* by $\Uparrow$, *backward* by $\Downarrow$, *left turn* by $\curvearrowleft$, and *right turn* by $\curvearrowright$. Thus the trajectory $\curvearrowleft\Uparrow\curvearrowleft$ can be read "left forward left". When necessary, a subscript will indicate the distance or angle traveled.

# 3 Controllability

Before applying Pontryagin's Maximum Principle to derive necessary conditions on optimal trajectories, we must show that trajectories exist for any given pair of start and goal states (controllability) and then that time optimal trajectories exist for any given pair of start and goal states.

To prove controllability we combine Equations 1, 2, 8, 10, and 11 to obtain

$$\begin{pmatrix} \dot{x} \\ \dot{y} \\ \dot{\theta} \end{pmatrix} = \omega_l f_l + \omega_r f_r \tag{12}$$

where $f_l$ and $f_r$ are the vector fields corresponding to the left and right wheels:

$$f_l = \begin{pmatrix} \frac{1}{2}\cos\theta \\ \frac{1}{2}\sin\theta \\ -\frac{1}{2b} \end{pmatrix} \tag{13}$$
$$f_r = \begin{pmatrix} \frac{1}{2}\cos\theta \\ \frac{1}{2}\sin\theta \\ \frac{1}{2b} \end{pmatrix} \tag{14}$$

Vector field $f_l$ corresponds to turning about a center located under the right wheel, and $f_r$ corresponds to turning about a center located under the left wheel.

We construct a third vector field which is the Lie bracket of $f_l$ and $f_r$:

$$f_{Lie} = [f_l, f_r] = Df_r\, f_l - Df_l\, f_r \tag{15}$$

where $Df$ is the Jacobian matrix, obtained by taking partials of the field $f$ with respect to the three state variables. Expanding these Jacobians and simplifying:

$$f_{Lie} = \begin{pmatrix} \frac{1}{2b}\sin\theta \\ -\frac{1}{2b}\cos\theta \\ 0 \end{pmatrix} \tag{16}$$

This third vector field corresponds to an infinitesimal parallel parking maneuver of the robot, translating the robot to its right. For nonzero $b$ it is readily observed that the three vector fields are linearly independent, satisfying the Lie Algebra Rank Condition. The diff drive robot is also symmetric, meaning that an admissible trajectory with time reversed yields an admissible trajectory. It follows from Theorem 2 of Sussman and Tang [6] that the bounded velocity diff drive robot is globally controllable, *i.e.* that admissible trajectories exist for every pair of start and goal configurations.

# 4 Existence of optimal trajectories.

**Theorem 1** *For any given start and goal configuration of a bounded velocity diff drive in the plane without obstacles, there is a time optimal control.*

*Proof:* Theorem 6 of Sussman and Tang [6] gives conditions sufficient for the existence of time optimal controls. For our case the conditions are:

- the system state variable $q = (x, y, \theta)$ takes values in an open subset of a differentiable manifold;
- the vector fields $f_l$ and $f_r$ are locally Lipschitz;
- the input $w = (\omega_l, \omega_r)$ takes values in a compact convex subset of $R^2$;
- the admissible controls are measurable functions on compact subintervals of $R$;
- for every start state and every control over some time interval, there is a trajectory starting at the start state, and defined over the whole interval.

The conditions are readily verified for the bounded velocity diff drive, and we know from Section 3 that trajectories exist for every pair of given start and goal states. It follows that time optimal controls exist for every given start and goal state. QED.

# 5 Pontryagin's Maximum Principle. Extremal controls.

This section uses Pontryagin's Maximum Principle [3] to derive necessary conditions for time optimal trajectories of the bounded velocity diff drive robot. The robot system is described by

$$\dot{q} = \begin{pmatrix} \dot{x} \\ \dot{y} \\ \dot{\theta} \end{pmatrix} = \begin{pmatrix} \frac{1}{2}(\omega_l + \omega_r)\cos(\theta) \\ \frac{1}{2}(\omega_l + \omega_r)\sin(\theta) \\ \frac{1}{2b}(\omega_r - \omega_l) \end{pmatrix} \tag{17}$$

where our input is

$$w = \begin{pmatrix} \omega_l \\ \omega_r \end{pmatrix} \in W$$

Define $\lambda$ to be an $R^3$-valued function of time called the *adjoint vector*:

$$\lambda(t) = \begin{pmatrix} \lambda_1(t) \\ \lambda_2(t) \\ \lambda_3(t) \end{pmatrix}$$

Let $H : R^3 \times SE^3 \times W \mapsto R$ be the *Hamiltonian*:

$$H(\lambda, q, w) = < \lambda, \omega_l f_l + \omega_r f_r >$$

where $f_l$ and $f_r$ are the vector fields defined by Equations 13 and 14.

The maximum principle states that for a control $w(t)$ to be optimal, it is *necessary* that there exist a nontrivial (not identically zero) adjoint vector $\lambda(t)$ satisfying the *adjoint equation*:

$$\dot{\lambda} \quad = \quad -\frac{\partial}{\partial q} H \tag{18}$$

while the control $w(t)$ minimizes the Hamiltonian at every $t$:

$$H(\lambda, q, w) \quad = \quad \min_{z \in W} H(\lambda, q, z) = \lambda_0. \tag{19}$$

with $\lambda_0 \geq 0$. Equation 18 is called the *adjoint equation* and Equation 19 is called the *minimization equation*.

For the bounded velocity diff drive, the adjoint equation gives

$$\begin{aligned} \dot{\lambda} \quad &= \quad -\frac{\partial}{\partial q} < \lambda, \omega_l f_l + \omega_r f_r > && (20) \\ &= \quad \frac{\omega_l + \omega_r}{2} \begin{pmatrix} 0 \\ 0 \\ \lambda_1 \sin\theta - \lambda_2 \cos\theta \end{pmatrix} && (21) \end{aligned}$$

Fortunately these equations can be integrated to obtain an expression for the adjoint vector. First we observe that $\lambda_1$ and $\lambda_2$ are constant and define $c_1$ and $c_2$ accordingly

$$\lambda_1(t) \quad = \quad c_1 \tag{22}$$

$$\lambda_2(t) \quad = \quad c_2 \tag{23}$$

For $\lambda_3$ we have the equation

$$\dot{\lambda}_3 = \frac{\omega_l + \omega_r}{2}(\lambda_1 \sin\theta - \lambda_2 \cos\theta) \tag{24}$$

But we can substitute from Equations 1, 10, and 11 to obtain

$$\dot{\lambda}_3 = c_1 \dot{y} - c_2 \dot{x} \tag{25}$$

which is integrated to obtain the solution for $\lambda_3$:

$$\lambda_3 = c_1 y - c_2 x + c_3 \tag{26}$$

where $c_3$ is our third and final integration constant. It will be convenient in the rest of the paper to define a function $\eta$ of $x$ and $y$:

$$\eta(x, y) = c_1 y - c_2 x + c_3 \tag{27}$$

So then the adjoint equation is satisfied by

$$\lambda = \begin{pmatrix} c_1 \\ c_2 \\ \eta(x, y) \end{pmatrix} \tag{28}$$

for any $c_1$, $c_2$, $c_3$ not all equal to zero.

Let the *$\eta$-line* to be the line of points $(x, y)$ satisfying $\eta(x, y) = 0$, and note that $\eta(x, y)$ gives a scaled directed distance of a point $(x, y)$ from the $\eta$-line. Let the *right half plane* be the points satisfying

$$\alpha x + \beta y + \gamma > 0 \tag{29}$$

and let the *left half plane* be the points satisfying

$$\alpha x + \beta y + \gamma < 0 \tag{30}$$

We also define a direction for the $\eta$-line consistent with our the choice of "left" and "right" for the half planes.

The minimization equation 19 can be rewritten

$$\omega_l \phi_l + \omega_r \phi_r = \min_{z_l, z_r} z_l \phi_l + z_r \phi_r \tag{31}$$

where $\phi_l$ and $\phi_r$ are defined to be the two *switching functions*:

$$\begin{aligned}
\phi_l &= <\lambda, f_l> && (32)\\
&= \begin{pmatrix} c_1 \\ c_2 \\ \eta(x, y, \theta) \end{pmatrix} \cdot \begin{pmatrix} \frac{1}{2}\cos\theta \\ \frac{1}{2}\sin\theta \\ -\frac{1}{2b} \end{pmatrix} && (33)\\
&= -\frac{1}{2b}\eta(x + b\sin\theta, y - b\cos\theta) && (34)\\
\phi_r &= <\lambda, f_r> && (35)\\
&= \begin{pmatrix} c_1 \\ c_2 \\ \eta(x, y, \theta) \end{pmatrix} \cdot \begin{pmatrix} \frac{1}{2}\cos\theta \\ \frac{1}{2}\sin\theta \\ \frac{1}{2b} \end{pmatrix} && (36)\\
&= \frac{1}{2b}\eta(x - b\sin\theta, y + b\cos\theta) && (37)
\end{aligned}$$

Note that the wheels' coordinates can be written

$$\begin{aligned}
\begin{pmatrix} x_l \\ y_l \end{pmatrix} &= \begin{pmatrix} x - b\sin\theta \\ y + b\cos\theta \end{pmatrix} && (38)\\
\begin{pmatrix} x_r \\ y_r \end{pmatrix} &= \begin{pmatrix} x + b\sin\theta \\ y - b\cos\theta \end{pmatrix} && (39)
\end{aligned}$$

so the switching functions can be written

$$\begin{aligned}
\phi_l &= -\frac{1}{2b}\eta(x_r, y_r) && (40)\\
\phi_r &= \frac{1}{2b}\eta(x_l, y_l) && (41)
\end{aligned}$$

Now the minimization equation says that if the controls $\omega_l, \omega_r$ are optimal then they minimize the Hamiltonian $H = \omega_l \phi_l + \omega_r \phi_r$ which implies the optimal controls can be expressed

$$\omega_l \begin{cases} = 1 & \text{if } \eta(x_r, y_r) > 0 \\ \in [-1, 1] & \text{if } \eta(x_r, y_r) = 0 \\ = -1 & \text{if } \eta(x_r, y_r) < 0 \end{cases} \tag{42}$$

$$\omega_r \begin{cases} = 1 & \text{if } \eta(x_l, y_l) < 0 \\ \in [-1, 1] & \text{if } \eta(x_l, y_l) = 0 \\ = -1 & \text{if } \eta(x_l, y_l) > 0 \end{cases} \tag{43}$$

These have a geometrical interpretation. We can restate Equations 42 and 43 as:

$$\omega_l \begin{cases} = 1 & \text{if right wheel} \in \text{right half plane} \\ \in [-1, 1] & \text{if right wheel} \in \eta\text{-line} \\ = -1 & \text{if right wheel} \in \text{left half plane} \end{cases} \tag{44}$$

$$\omega_r \begin{cases} = 1 & \text{if left wheel} \in \text{left half plane} \\ \in [-1, 1] & \text{if left wheel} \in \eta\text{-line} \\ = -1 & \text{if left wheel} \in \text{right half plane} \end{cases} \tag{45}$$

If $c_1 = c_2 = 0$, then the $\eta$-line is at infinity, and the entire plane is the left half plane or the right half plane, depending on the sign of $c_3$. (Recall that all three integration constants cannot be simultaneously zero.)

The location of the $\eta$-line depends on the apparently arbitrary integration constants. The maximum principle does not give the location of the line; it merely says that if we have an optimal control then the line exists and the optimal control must conform to the equations above. The question that naturally arises is how to locate the line properly, given the start and goal configurations of the robot. There seems to be no direct way of doing so. Rather, we must use other means to identify the extremal trajectory.

The behavior of the robot falls into one of the following cases (Figure 1):

- `CCW` and `CW`: If the robot is in the left half plane and out of reach of the $\eta$-line, it turns in the counterclockwise direction (`CCW`). `CW` is similar.

- `TCCW` and `TCW` (Tangent CCW and Tangent CW). If the robot is in the left half plane, but close enough that a circumscribed circle is tangent to the $\eta$-line, then the robot may either roll straight along the line, or it may turn through any positive multiple of $\pi$. `TCW` is similar.

- ZR and ZL: If the circumscribed circle crosses the $\eta$-line, then a zigzag behavior occurs. The robot rolls straight in the $\eta$-line's direction until one wheel crosses. It then turns until the other wheel crosses, and then goes straight again. There are two non-degenerate patterns: ... ⇑↶⇓↷ ... called *zigzag right* ZR, and ... ⇑↷⇓↶ ... called *zigzag left* ZL.

Every nontrivial time-optimal control must fall in one of the above cases. However, the converse is definitely not true—not every trajectory conforming to the cases above is optimal. To keep the distinction clear, we refer to trajectories satisfying Pontryagin's Maximum Principle as *extremal*, and we note that the time-optimal trajectories are a subset of the extremal trajectories.

# 6 Further necessary conditions. Symmetries. Enumeration.

We note above that not all extremals are optimal. For example, a robot turning in place for several revolutions is not time optimal. Further, a zigzag of a hundred segments is not optimal. In fact, it can be shown that the magnitudes of all the turns of an optimal trajectory never sums to more than $\pi$ radians, that optimal trajectories of class TCW or TCCW have at most three segments, and that optimal trajectories of class ZR and ZL have at most 5 segments. This gives us a finite enumeration of a reduced set of extremals that still includes all optimal trajectories.

We can reduce the number of cases by employing symmetries developed by Souères, Boissonnat, and Laumond [4, 5].

The symmetries are summarized in Figure 4. Let $\tau$ be an extremal trajectory from $q = (x, y, \theta)$ to the origin. Then there are seven other trajectories, obtained by applying one or more of three transformations defined below. Geometrically, the transformations reflect the plane across the origin or across one of three other lines: the $x$-axis, a line $\Delta_\theta$ at angle $(\pi + \theta_s)/2$, or the line $\Delta_\theta^\perp$ at angle $\theta_s/2$.

The three transformations are:

- Let $\tau_1(\tau)$ be the trajectory obtained by switching the directions of straights, i.e. switching $\Downarrow$ and $\Uparrow$. Let $T_1([x, y, \theta]) = [-x, -y, \theta]$. $\tau$ is optimal from $q$ if and only if $\tau_1(\tau)$ is optimal from $T_1(q)$.

- Let $\tau_2(\tau)$ be the trajectory obtained by reversing the order of the segments. Let $T_2([x, y, \theta]) = [x', y', \theta]$ where $[x', y'] = \mathrm{Rot}(\theta)[x, -y]$. $\tau$ is optimal from $q$ if and only if $\tau_2(\tau)$ is optimal from $T_2(q)$.

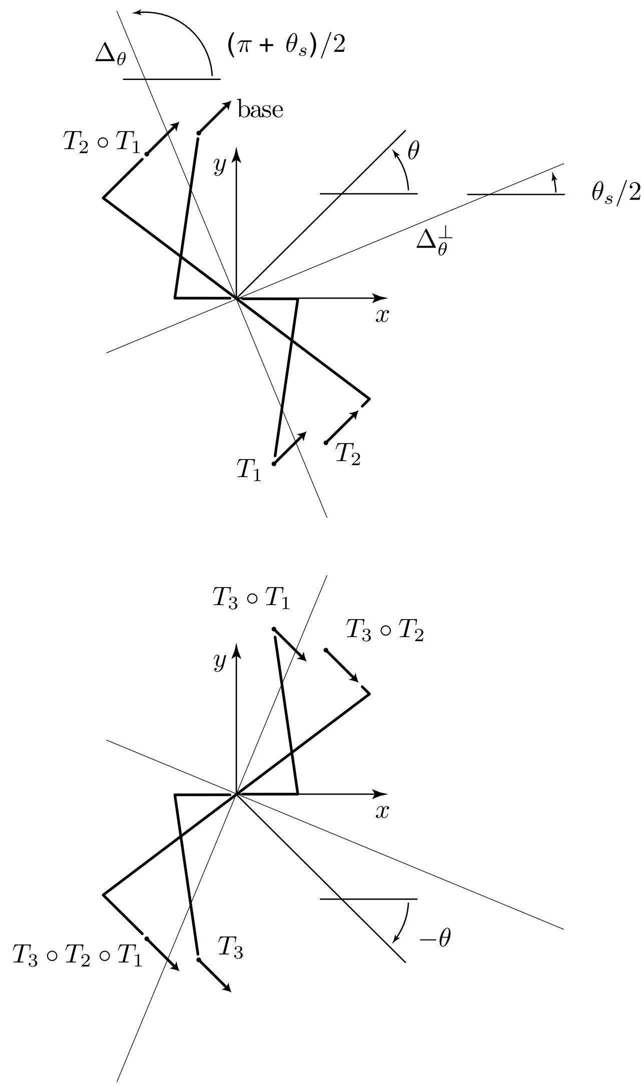


Figure 4: Given an optimal trajectory from "base" with heading $\theta_s$ to the origin with heading $\theta_g = 0$, transformations $T_1$,$T_2$, and $T_3$ yield up to seven other optimal trajectories symmetric to the original. symmetries.

- Let $\tau_3(\tau)$ be the trajectory obtained by switching the directions of turns, i.e. switching $\curvearrowright$ and $\curvearrowleft$. Let $T_3([x, y, \theta]) = [x, -y, -\theta]$. $\tau$ is optimal from $q$ if and only if $\tau_3(\tau)$ is optimal from $T_3(q)$.

It is evident from the definitions that each transformation is its own inverse, and that the three transformations commute. For any given base trajectory, the transformations yield up to seven different symmetric trajectories. The result is that all optimal trajectories fall in one of 9 symmetry classes.

| | base | $T_1$ | $T_2$ | $T_2 \circ T_1$ |
|---|---|---|---|---|
| A. | $\Uparrow\curvearrowleft\Downarrow\curvearrowright\Uparrow$ | $\Downarrow\curvearrowleft\Uparrow\curvearrowright\Downarrow$ | $\Uparrow\curvearrowright\Downarrow\curvearrowleft\Uparrow$ | $\Downarrow\curvearrowright\Uparrow\curvearrowleft\Downarrow$ |
| B. | $\curvearrowleft\Downarrow\curvearrowright\Uparrow$ | $\curvearrowleft\Uparrow\curvearrowright\Downarrow$ | $\Uparrow\curvearrowright\Downarrow\curvearrowleft$ | $\Downarrow\curvearrowright\Uparrow\curvearrowleft$ |
| C. | $\Downarrow\curvearrowright\Uparrow$ | $\Uparrow\curvearrowright\Downarrow$ | $\Uparrow\curvearrowright\Downarrow$ | $\Downarrow\curvearrowright\Uparrow$ |
| D. | $\Uparrow\curvearrowleft_{\pi}\Downarrow$ | $\Downarrow\curvearrowleft_{\pi}\Uparrow$ | $\Downarrow\curvearrowleft_{\pi}\Uparrow$ | $\Uparrow\curvearrowleft_{\pi}\Downarrow$ |
| E. | $\curvearrowright\Downarrow\curvearrowright$ | $\curvearrowright\Uparrow\curvearrowright$ | $\curvearrowright\Downarrow\curvearrowright$ | $\curvearrowright\Uparrow\curvearrowright$ |
| F. | $\curvearrowleft\Downarrow\curvearrowright$ | $\curvearrowleft\Uparrow\curvearrowright$ | $\curvearrowright\Downarrow\curvearrowleft$ | $\curvearrowright\Uparrow\curvearrowleft$ |
| G. | $\Downarrow\curvearrowright$ | $\Uparrow\curvearrowright$ | $\curvearrowright\Downarrow$ | $\curvearrowright\Uparrow$ |
| H. | $\Downarrow$ | $\Uparrow$ | $\Downarrow$ | $\Uparrow$ |
| I. | $\curvearrowright$ | $\curvearrowright$ | $\curvearrowright$ | $\curvearrowright$ |

| | $T_3$ | $T_3 \circ T_1$ | $T_3 \circ T_2$ | $T_3 \circ T_2 \circ T_1$ |
|---|---|---|---|---|
| A. | $\Uparrow\curvearrowright\Downarrow\curvearrowleft\Uparrow$ | $\Downarrow\curvearrowright\Uparrow\curvearrowleft\Downarrow$ | $\Uparrow\curvearrowleft\Downarrow\curvearrowright\Uparrow$ | $\Downarrow\curvearrowleft\Uparrow\curvearrowright\Downarrow$ |
| B. | $\curvearrowright\Downarrow\curvearrowleft\Uparrow$ | $\curvearrowright\Uparrow\curvearrowleft\Downarrow$ | $\Uparrow\curvearrowleft\Downarrow\curvearrowright$ | $\Downarrow\curvearrowleft\Uparrow\curvearrowright$ |
| C. | $\Downarrow\curvearrowleft\Uparrow$ | $\Uparrow\curvearrowleft\Downarrow$ | $\Uparrow\curvearrowleft\Downarrow$ | $\Downarrow\curvearrowleft\Uparrow$ |
| D. | $\Uparrow\curvearrowright_{-\pi}\Downarrow$ | $\Downarrow\curvearrowright_{-\pi}\Uparrow$ | $\Downarrow\curvearrowright_{-\pi}\Uparrow$ | $\Uparrow\curvearrowright_{-\pi}\Downarrow$ |
| E. | $\curvearrowleft\Downarrow\curvearrowleft$ | $\curvearrowleft\Uparrow\curvearrowleft$ | $\curvearrowleft\Downarrow\curvearrowleft$ | $\curvearrowleft\Uparrow\curvearrowleft$ |
| F. | $\curvearrowright\Downarrow\curvearrowleft$ | $\curvearrowright\Uparrow\curvearrowleft$ | $\curvearrowleft\Downarrow\curvearrowright$ | $\curvearrowleft\Uparrow\curvearrowright$ |
| G. | $\Downarrow\curvearrowleft$ | $\Uparrow\curvearrowleft$ | $\curvearrowleft\Downarrow$ | $\curvearrowleft\Uparrow$ |
| H. | $\Downarrow$ | $\Uparrow$ | $\Downarrow$ | $\Uparrow$ |
| I. | $\curvearrowleft$ | $\curvearrowleft$ | $\curvearrowleft$ | $\curvearrowleft$ |

We can analyze all types of trajectories by analyzing just one type from each of the nine classes, and then applying the transformations $T_1, T_2, T_3$ to obtain the other members of the class. The number of cases can be further reduced by noticing that classes D, G, H, and I can be treated as degenerate or limiting cases of classes B, C, E, and F. Class A, consisting of five-segment trajectories that are optimal only when $\theta_s = \theta_g$, is also easily analyzed as it only occurs when two different members of class B are valid. Thus we have obtained a reduced set of extremal trajectories, which still includes all optimal trajectories, which can be analyzed by considering just four cases.

# 7 Summary and Conclusion.

This paper analyzed the bounded velocity differential drive model using Pontryagin's Maximum Principle. The Maximum Principle provides an elegant geomtric program that generates all optimal trajectories. Further necessary conditions and the use of symmetries reduces the number of cases to just four.

## Acknowledgments

The authors wish to thank Jean-Paul Laumond for encouragement and guidance throughout the project. We would also like to thank Al Rizzi, Howie Choset, Ercan Acar, and members of the Manipulation Lab for comments and discussion.

# References

[1] D. J. Balkcom and M. T. Mason. Time optimal trajectories for bounded velocity differential drive robots. In *IEEE International Conference on Robotics and Automation*, 2000. submitted.

[2] J.-D. Boissonnat, A. Cérézo, and J. Leblond. Shortest paths of bounded curvature in the plane. In *Proceedings of the 1992 International Conference on Robotics and Automation*, pages 2315–2320, 1992.

[3] L. S. Pontryagin, V. G. Boltyanskii, R. V. Gamkrelidze, and E. F. Mishchenko. *The Mathematical Theory of Optimal Processes*. John Wiley, 1962.

[4] P. Souères and J.-D. Boissonnat. Optimal trajectories for nonholonomic mobile robots. In J.-P. Laumond, editor, *Robot Motion Planning and Control*, pages 93–170. Springer, 1998.

[5] P. Souères and J.-P. Laumond. Shortest paths synthesis for a car-like robot. *IEEE Transactions on Automatic Control*, 41(5):672–688, May 1996.

[6] H. Sussmann and G. Tang. Shortest paths for the reeds-shepp car: a worked out example of the use of geometric techniques in nonlinear optimal control. SYCON 91-10, Department of Mathematics, Rutgers University, New Brunswick, NJ 08903, 1991.